

Supporting Information

Investigating the Electroactivity of Nitrogen Species in MoC Nanoparticle/N-doped Carbon Nanosheets for High-performance Na/Li-ion batteries

Qing Wu, Xiaofeng Li, Xianjie Wang, Tai Yao, Ying Bai, Jikang Jian, and Bo Song*

Part I: Computational Methods

The detailed calculation processes of pseudocapacitance according to CV curves at different scan rates.

For Fig. 3a and 3b, the contributions from diffusion and capacitive processes can be qualitatively evaluated during the sodium ion storage process through the following formula S-1¹

$$i = av^b \quad (\text{S-1})$$

where i is the current response at a particular voltage; v is the scan rate; a and b are adjustable value, and the value can be worked out by fitted the $\log(v)$ - $\log(i)$ plots. The b values of 0.5 and 1 reveal the diffusion-controlled process and capacitive-controlled process, respectively.² Fig. 3b shows the plots of log (peak current) versus log (scan rate) at different redox states, and the linear fitting indicates the slopes (b) of the anodic (peak 1) and cathodic (peak 2) peaks are 0.98 and 0.93, respectively.

According to the following equation S-2³

$$i = k_1v + k_2v^{1/2} \quad (\text{S-2})$$

the ratios of capacitive contribution (k_1v) and diffusion contribution ($k_2v^{1/2}$) could be quantitatively determined.⁴ The relative capacitive contributions at different scan rates are quantified as 37%, 48%, 51%, 56%, and 60% at scan rates of 0.2, 0.4, 0.6, 0.8, and 1.0 mV s⁻¹, respectively (Fig. 3c).

The detailed calculation processes of diffusion coefficient according to electrochemical impedance spectroscopy (EIS).

The Na-ion diffusion coefficient could be obtained by the following formula:⁵

$$D = \frac{1}{2} \left(\frac{RT}{An^2 F^2 C\sigma} \right)^2 \quad (\text{S-3})$$

According to this formula, R represents the gas constant, T represents the experiment temperature, F represents the Faraday constant. A represents the electrode surface area, n means the electrons per molecule involving in the reaction, and C represents the sodium ions concentration in the electrode. The σ is the Warburg coefficient which could be calculated by the gradient of the oblique line $Z' \sim \omega^{-1/2}$ ($\omega = 2\pi f$) in the low-frequency area (Fig. S3).

Herein, the D values of MoC@NC electrodes are compared in Table S3.

Part II: Figures

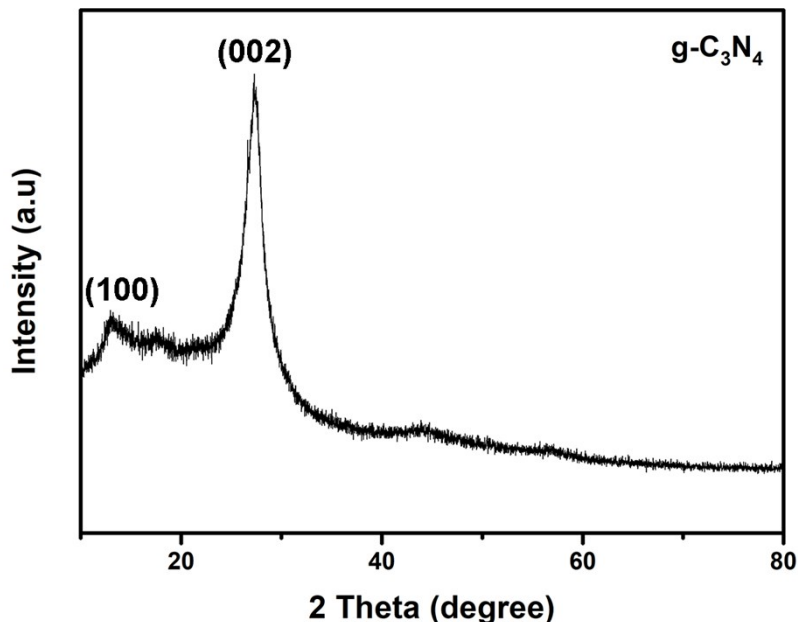


Fig. S1 XRD pattern of $g\text{-C}_3\text{N}_4$

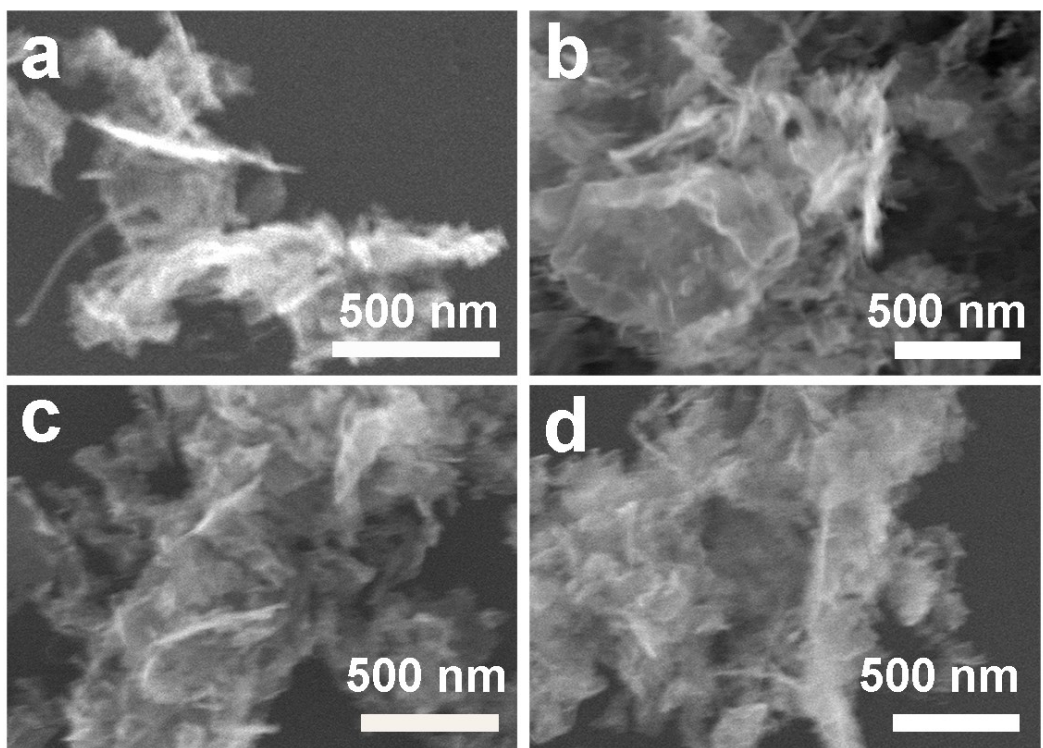


Fig. S2 SEM images of a) MoC@NC-0.5, b) MoC@NC-0.75, c) MoC@NC-1.0, d) MoC@NC-1.25.

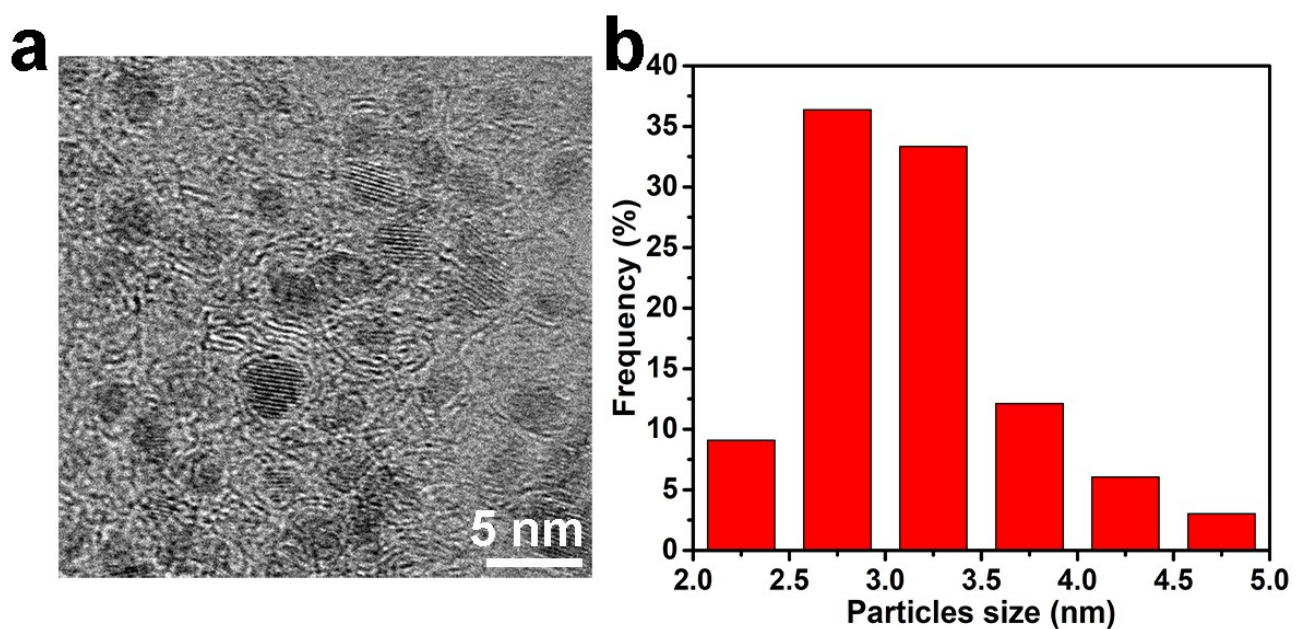


Fig. S3 a) HRTEM image and b) The corresponding size distribution of MoC NPs.

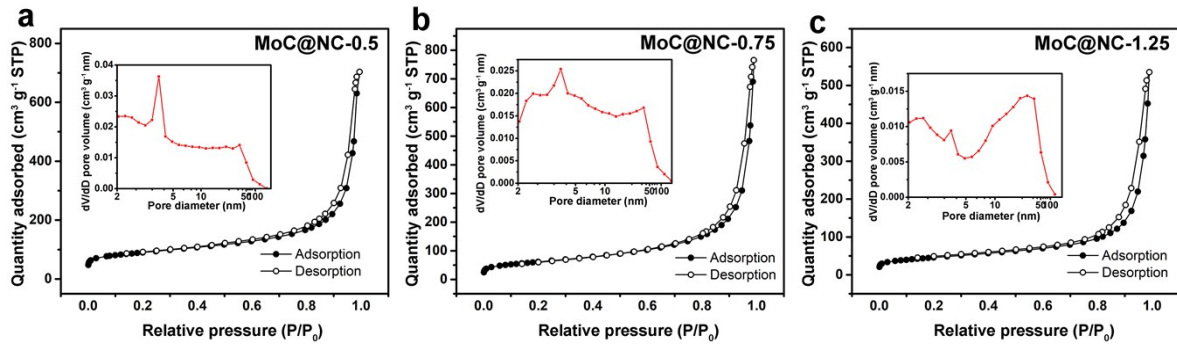


Fig. S4 N₂ sorption isotherms and pore size distribution of a) MoC@NC-0.5, b) MoC@NC-0.75, c) MoC@NC-1.25

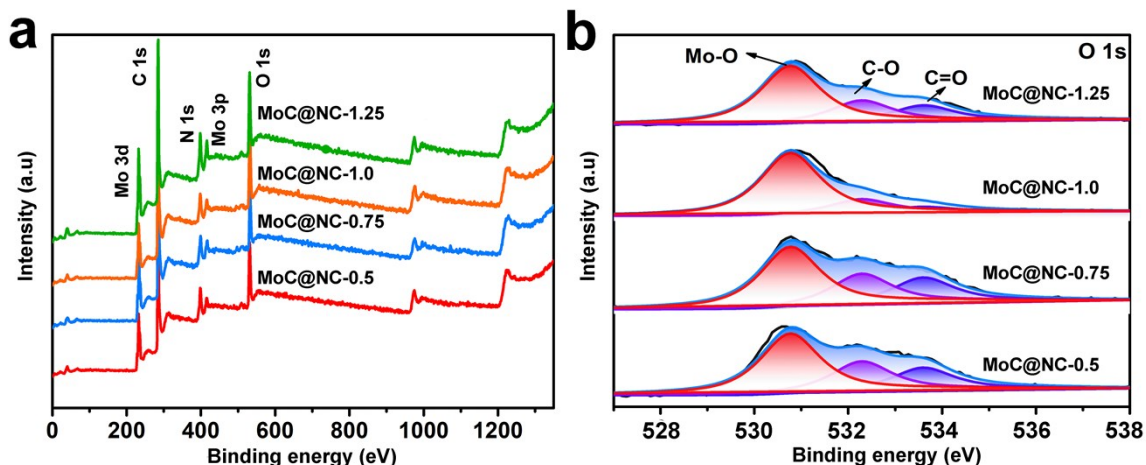


Fig. S5 XPS spectra of MoC@NCs a) Survey spectra, b) O 1s.

The full range XPS survey spectra (Fig. S5) involve five distinct peaks of Mo 3d at \sim 232 eV, C 1s at \sim 285 eV, N 1s at \sim 398 eV, Mo 3p at \sim 413 eV and O 1s at \sim 530 eV. The presence of oxygen element is likely due to the physically adsorbed and/or trapped oxygen and moisture on the surfaces of samples, or the small amount of oxygen-containing functional group as generated during the synthesis process.⁶⁻⁸

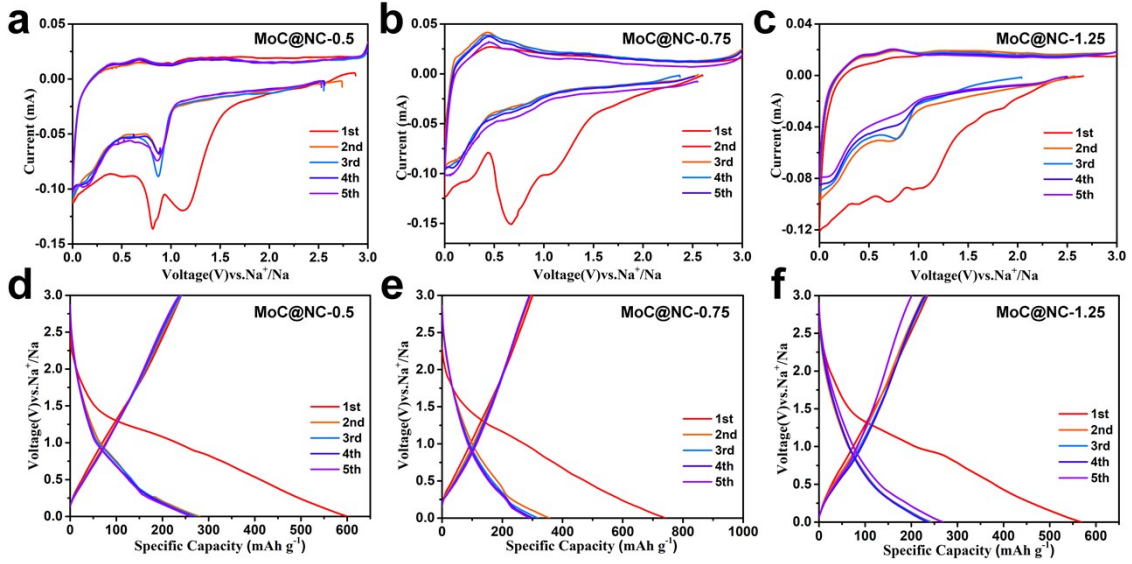


Fig. S6 Electrochemical performances of MoC@NC electrodes in Na-ion half cells. a)-c) CV curves at 0.1 mV s^{-1} and d)-f) Charge/discharge curves of the initial 5 cycles at 0.1 A g^{-1} .

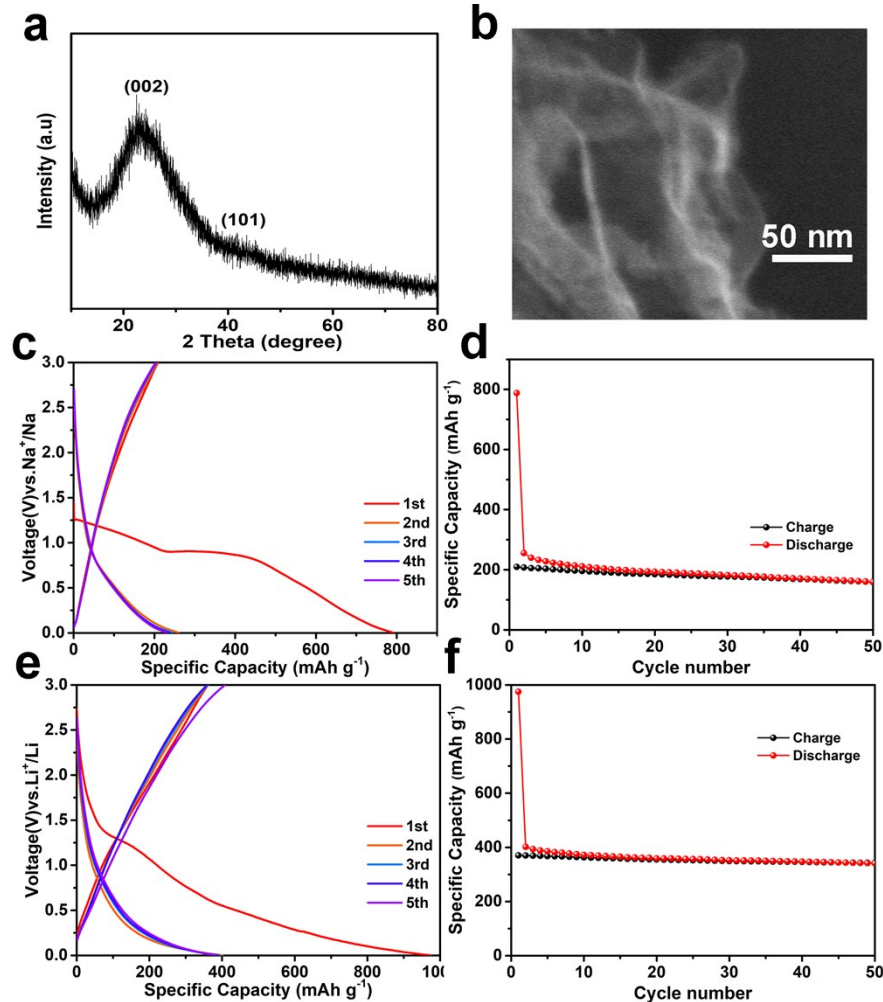


Fig. S7 a) XRD pattern and b) SEM image of the bare N doped carbon NSs. Charge/discharge curves of the first 5 cycles at 0.1 A g^{-1} and cycling stability of the bare N doped carbon NSs in sodium ion half cells (c) and (d) and lithium ion half cells (e) and (f).

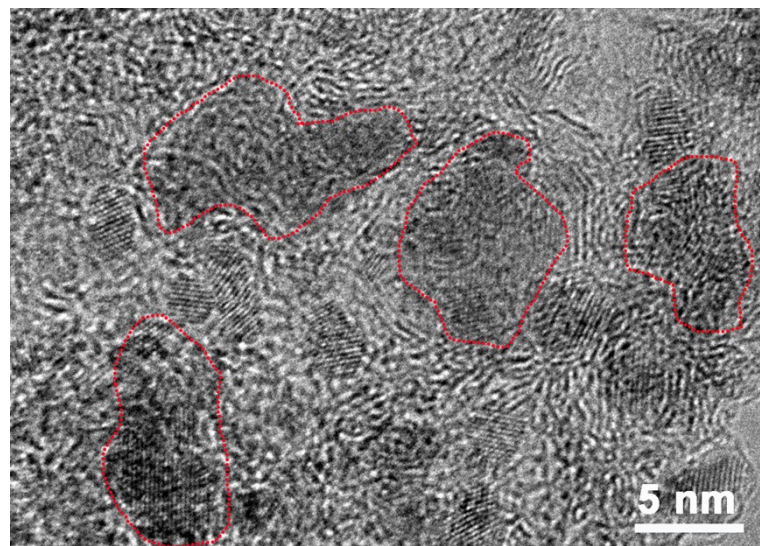


Fig. S8 a) HRTEM image of MoC@NC-1.25.

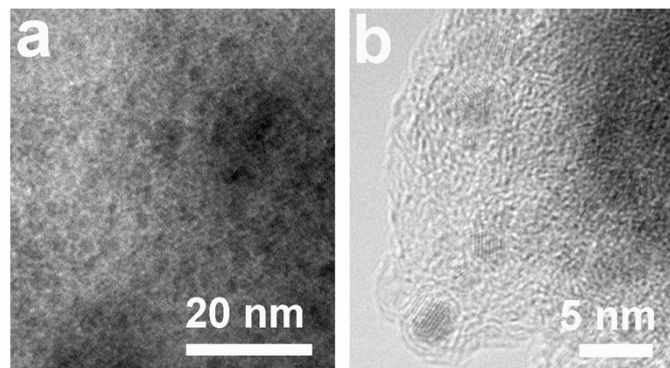


Fig. S9 a) TEM and b) HRTEM images of MoC@NC-1.0 electrode after 50 cycles in SIBs.

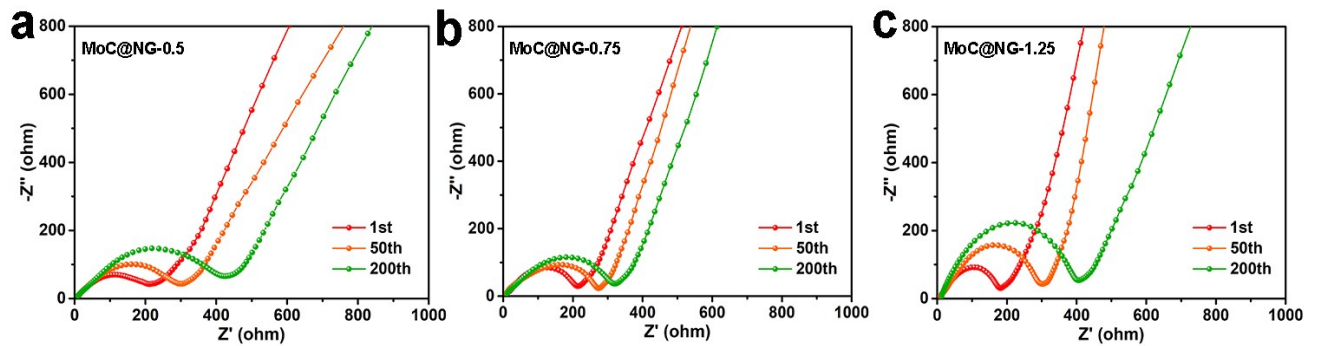


Fig. S10 Nyquist plots of a) MoC@NC-0.5, b) MoC@NC-0.75 and c) MoC@NC-1.25 electrodes after 1, 50 and 200 cycles in the fully charged state.

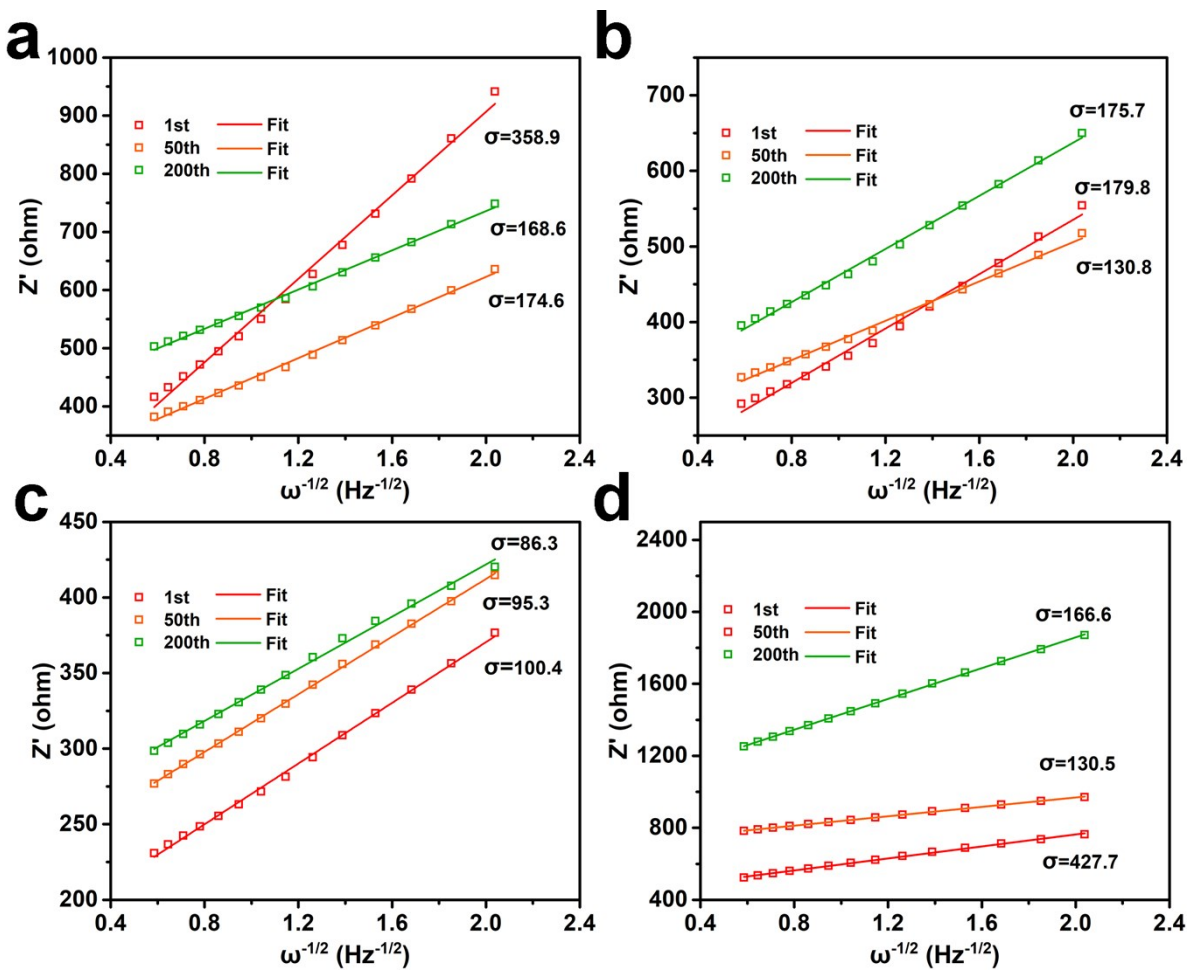


Fig. S11 Plots of $\omega^{1/2}$ versus Z' in the low-frequency region for 1st, 50th and 200th cycles of a) MoC@NC-0.5, b) MoC@NC-0.75, c) MoC@NC-1.0 and d) MoC@NC-1.25.

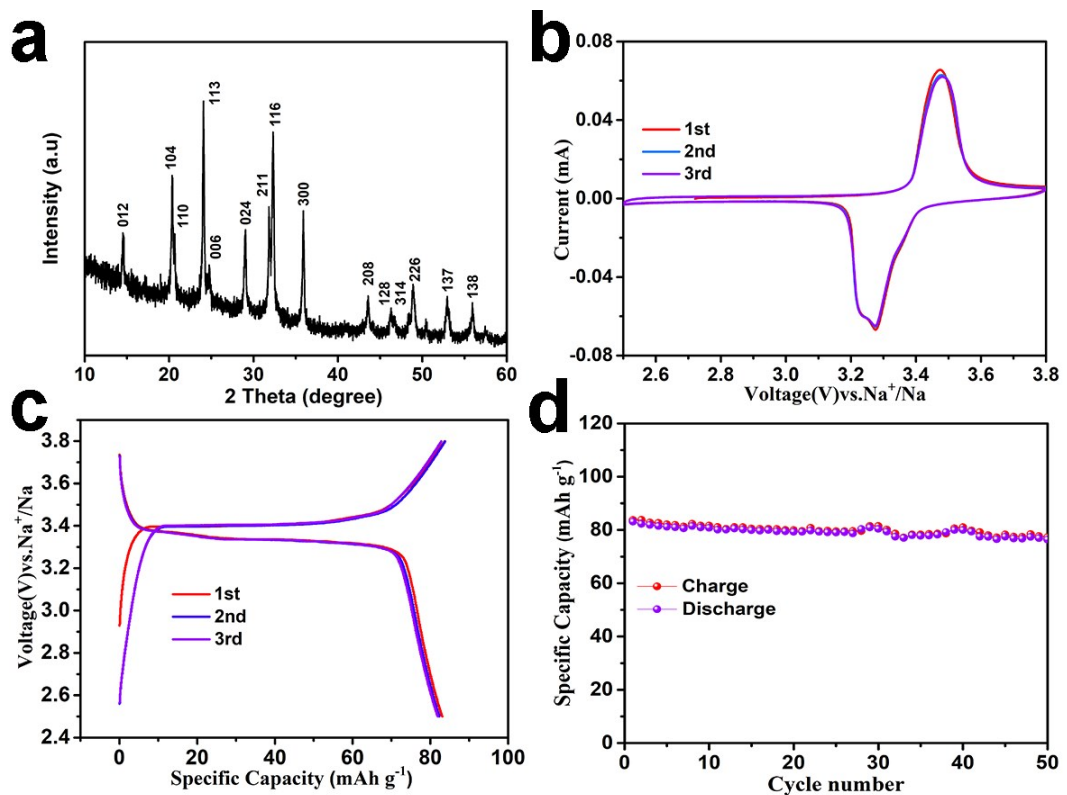


Fig. S12 XRD pattern of the as-prepared NVP. b) Cyclic voltammograms of NVP at a scan rate of 0.1 mV s^{-1} . c) Charge/discharge curves and d) Cycling performance of NVP material at a current density of 0.1 C .

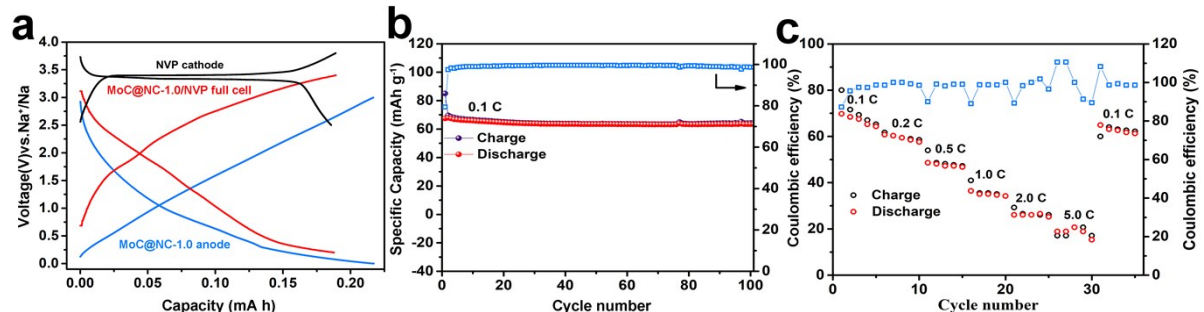


Fig. S13 a) The galvanostatic charge/discharge profiles of sodium-ion MoC@NC-1.0/NVP full cell and the corresponding NVP cathode and MoC@NC-1.0 anode in half cells. b) Cycling stability and c) Rate performance of MoC@NC-1.0/NVP cell.

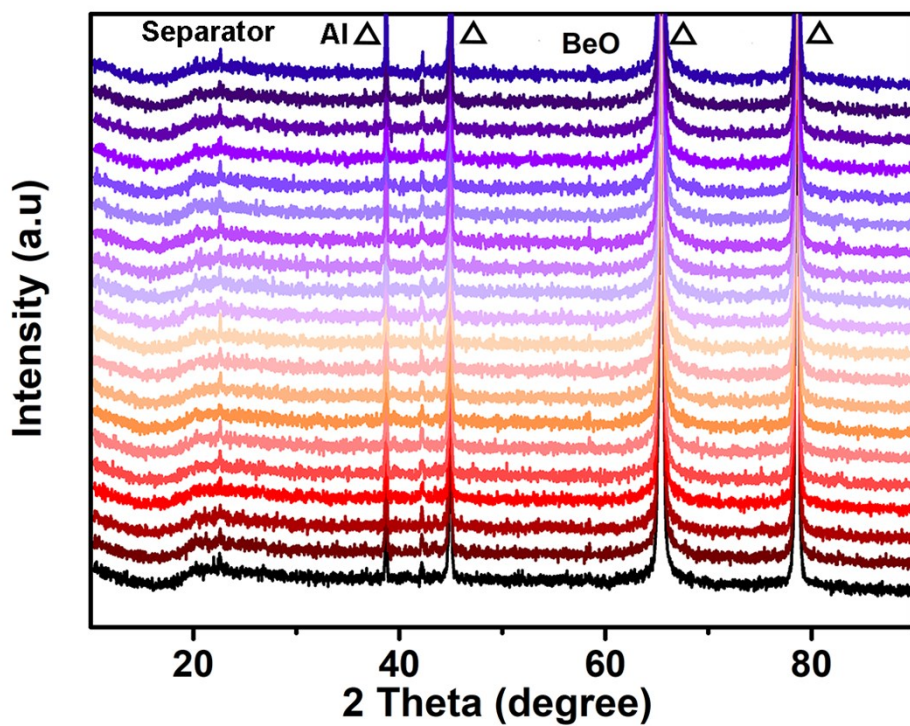


Fig. S14 The evolution of *in situ* XRD patterns of MoC@NC-1.0 electrode during the first charge/discharge process (versus Na/Na⁺).

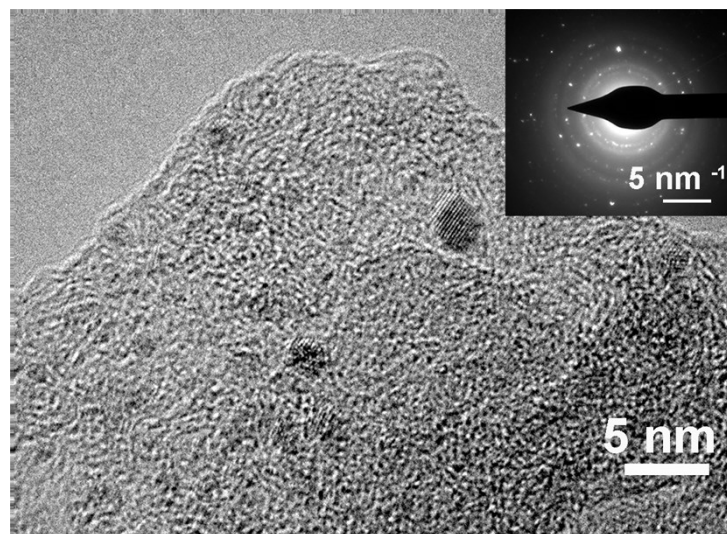


Fig. S15 HRTEM image and the corresponding SAED pattern (inset in Fig.S15) of MoC@NC-1.0 electrode after 50 cycles.

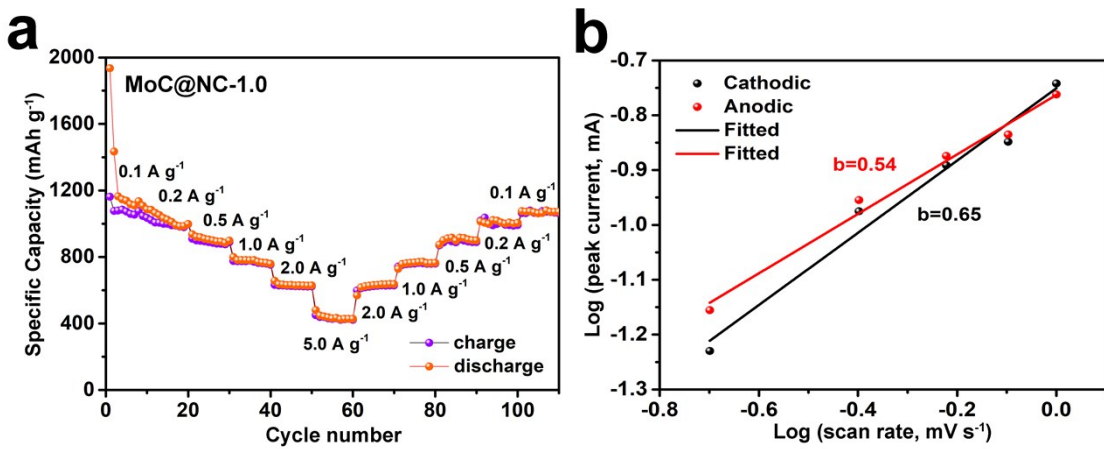


Fig. S16 Electrochemical performances of the MoC@NC-1.0 electrode in LIBs. a) Rate performance of MoC@NC-1.0 at various current densities. b) Calculated b values for the anodic scan and cathodic scan.

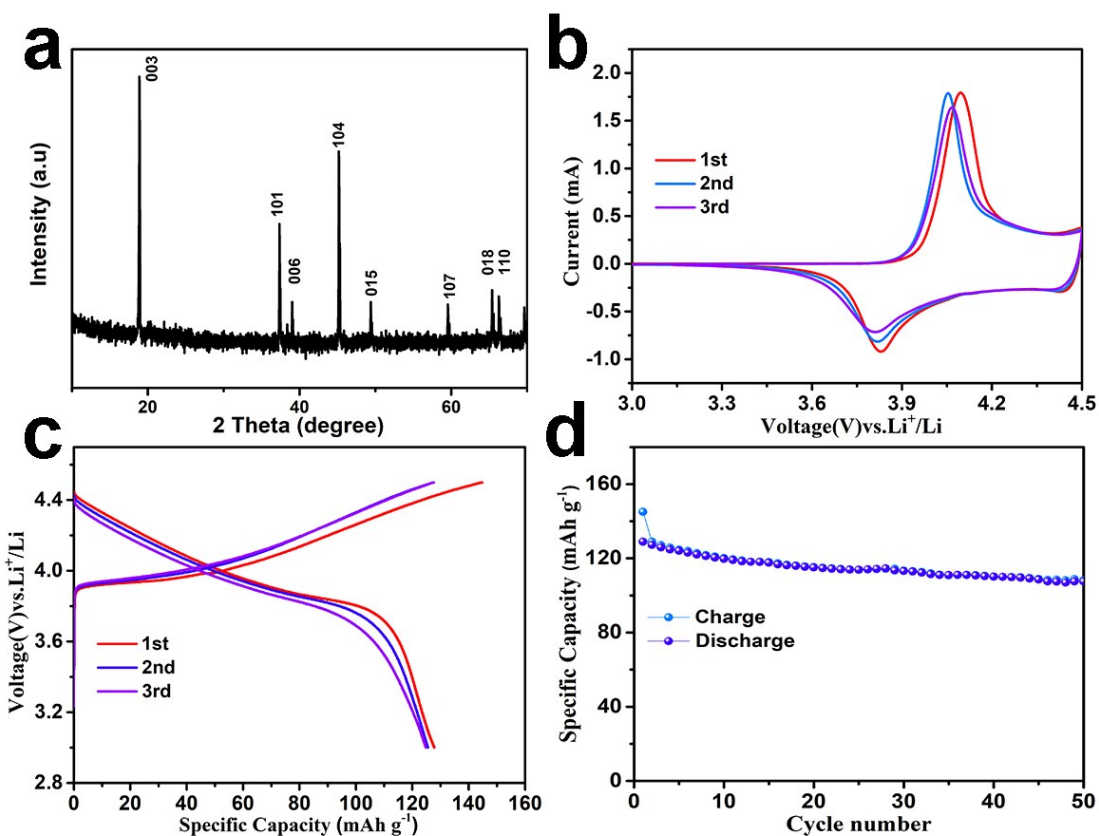


Fig. S17 a) XRD pattern of the as-prepared LCO. b) Cyclic voltammograms of LCO at a scan rate of 0.1 mV s^{-1} . c) Charge/discharge curves and d) Cycling performance of LCO material at a current density of 0.1 C .

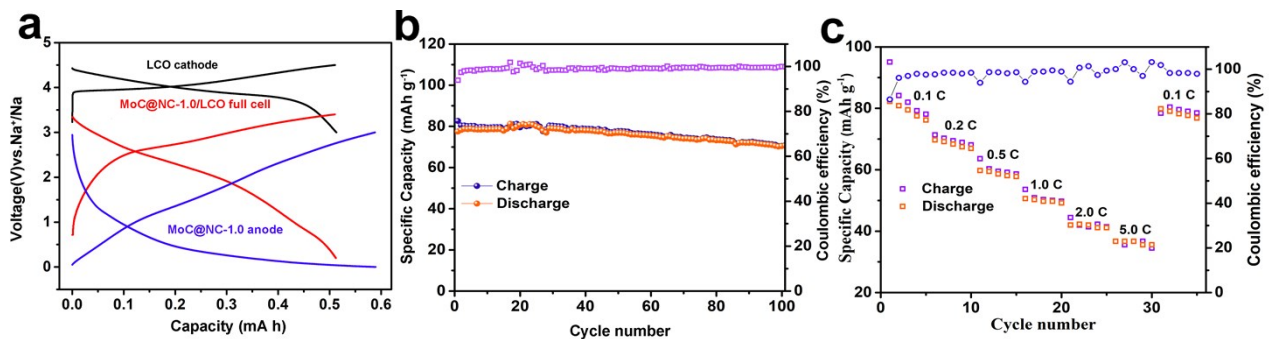


Fig. S18 a) The galvanostatic charge/discharge profiles of lithium-ion MoC@NC-1.0/LCO full cell and the corresponding LCO cathode and MoC@NC-1.0 anode in half cells. b) Cycling performance and c) Rate performance of MoC@NC-1.0/LCO full cell.

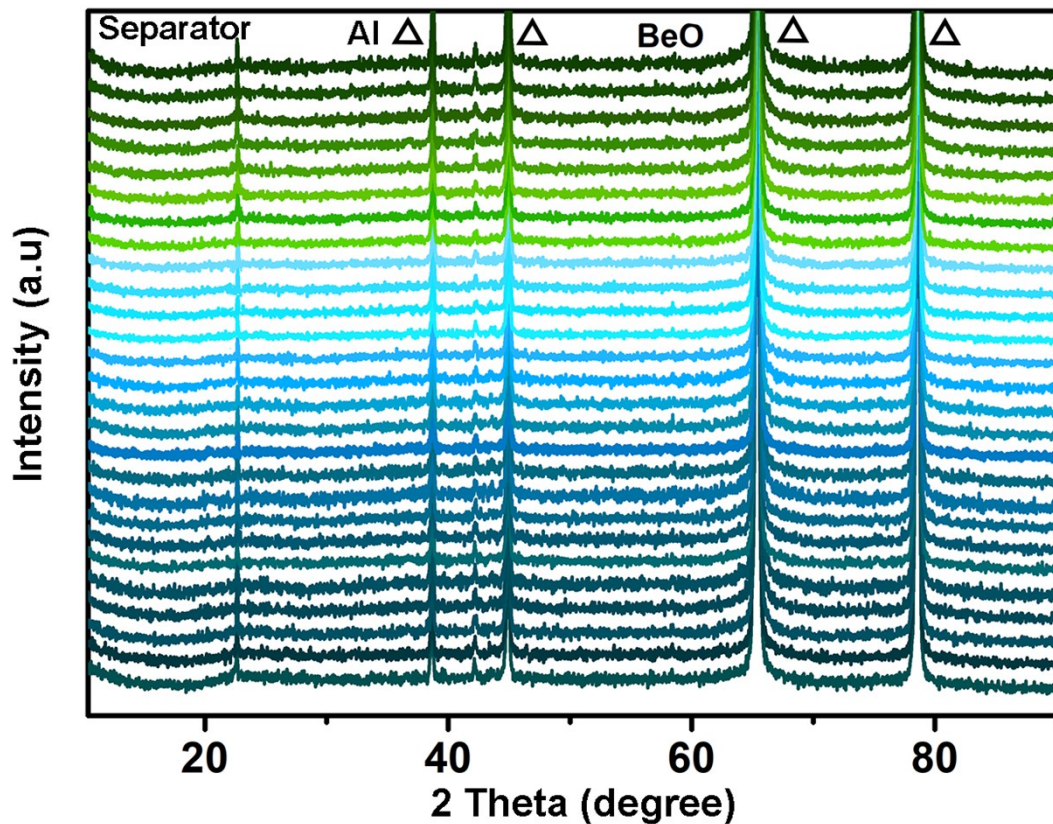


Fig. S19 The *in situ* XRD patterns of the MoC@NC-1.0 electrode during the initial cycle (versus Li/Li⁺).

Part III : Tables

Table S1 Elemental compositions of MoC@NC electrodes.

Samples	Mo_{xps} (At%)	C_{xps} (At%)	N_{xps} (At%)	O_{xps} (At%)
MoC@NC-0.5	2.44	74.77	8.66	14.14
MoC@NC-0.75	2.98	75.35	10.26	11.41
MoC@NC-1.0	4.05	68.3	15.89	11.77
MoC@NC-1.25	4.29	65.5	15.07	15.15

Table S2 The electronic conductivity of the as-prepared samples.

Samples	electronic conductivity (S/m)		
	1 MPa	2 MPa	3 MPa
MoC@NC-0.5	10.14	12.08	15.93
MoC@NC-0.75	13.38	20.62	25.58
MoC@NC-1.0	31.25	31.65	31.95
MoC@NC-1.25	19.8	30.04	30.74

Table S3. Comparison of cycling stability of molybdenum carbides-based anode materials for SIBs.

Materials	Cycling stability performance				
	Current	Capasity (mAh g ⁻¹)	cycles	Capacity retation	Referenc e
MoC@NC-1.0	0.1 A g⁻¹	340	200	88%	This work
	1.0 A g⁻¹	245	1000	98%	
MoC@C ₃ N ₄	0.16 A g ⁻¹	410	200	0.66%	9
	0.5 A g ⁻¹	310	/	/	
Mo ₂ C nanoplates	0.2 A g ⁻¹	90.8	400	76%	10
	0.5 A g ⁻¹	75	400	75%	

3D Macroporous MXene Mo ₂ CT _x	0.25 C 2.5 C	370 290	/	/	11
MoC/graphitic nanocomposites	0.05 A g ⁻¹ 0.2 A g ⁻¹	250 200	50	83%	12
Mo ₂ C/N-doped carbon nanowires	0.05 A g ⁻¹ 0.5 A g ⁻¹	166 167	100	54%	13
			/	/	

Table S4 EIS data of MoC@NC electrodes.

Samples	1st	50th	200th
MoC@NC-0.5	220	310	435
MoC@NC-0.75	213	272	325
MoC@NC-1.0	172	227	262
MoC@NC-1.25	184	304	408

Table S5 The diffusion coefficients of MoC@NC electrodes at different cycles.

Samples	Cycles	MoC@NC-0.5	MoC@NC-0.75	MoC@NC-1.0	MoC@NC-1.25
D _{Na+} [cm ² s ⁻¹]	1st	2.45×10 ⁻¹⁴	4.89×10 ⁻¹⁴	8.75×10 ⁻¹⁴	5.27×10 ⁻¹⁴
	50th	4.64×10 ⁻¹⁴	6.71×10 ⁻¹⁴	9.20×10 ⁻¹⁴	6.73×10 ⁻¹⁴
	200th	5.20×10 ⁻¹⁴	5.0×10 ⁻¹⁴	1.02×10 ⁻¹³	2.0×10 ⁻¹⁴

Table S6 Comparison of rate performance of molybdenum carbides-based anode materials for LIBs.

Materials	Rate performance				Referenc e
	Current	Capasity (mAh g ⁻¹)	Current	Capasity (mAh g ⁻¹)	
MoC@NC-1.0	0.1 A g⁻¹	1062	0.2 A g⁻¹	893	This work

	1.0 A g⁻¹	768	5.0 A g⁻¹	422	
3D ordered porous MoC	0.2 A g ⁻¹	912	1.0 A g ⁻¹	738.3	¹⁴
Mo ₂ C/C Hollow Spheres	0.1 A g ⁻¹	933	0.2 A g ⁻¹	873	¹⁵
	1.0 A g ⁻¹	667	2.0 A g ⁻¹	546	
Mo ₂ C/C	0.1 A g ⁻¹	780	0.2 A g ⁻¹	700	¹⁶
	0.5 A g ⁻¹	625	1.0 A g ⁻¹	550	
η -MoC/MXene/C	0.2 A g ⁻¹	820	2.0 A g ⁻¹	750	¹⁷
	5.0 A g ⁻¹	720	20.0 A g ⁻¹	700	
3D Macroporous Mo _x C@N-C	0.1 A g ⁻¹	838	0.25 A g ⁻¹	728	¹⁸
	1.0 A g ⁻¹	535	5.0 A g ⁻¹	266	
MoC _{1-x} Nanodot@Carbon	0.1 A g ⁻¹	920	0.2 A g ⁻¹	750	¹⁹
	1.0 A g ⁻¹	657	5.0 A g ⁻¹	400	
N, P Co-Doped Mo ₂ C/C NSs	0.15 A g ⁻¹	863	0.45 A g ⁻¹	793	²⁰
	1.5 A g ⁻¹	708.5	3.0 A g ⁻¹	648.1	

References

1. C. Zhao, C. Yu, M. Zhang, H. Huang, S. Li, X. Han, Z. Liu, J. Yang, W. Xiao, J. Liang, X. Sun and J. Qiu, *Adv. Energy Mater.*, 2017, **7**, 1602880.
2. J. W. Torsten Brezesinski, Julien Polleux, Bruce Dunn and Sarah H. Tolbert, *J. Am. Chem. Soc.*, 2009, **131**, 1802–1809.
3. P. Yu, C. Li and X. Guo, *J. Phys.Chem. C*, 2014, **118**, 10616-10624.
4. J. P. John Wang, J. Lim and Bruce Dunn, *J. Phys. Chem. C* 2007, **111**, 14925-14931.
5. Z. Ju, P. Li, G. Ma, Z. Xing, Q. Zhuang and Y. Qian, *Energy Storage Mater.*, 2018, **11**, 38-46.
6. P. Xiao, L. Thia, X. Ge, R. Lim, J. Wang, K. Lima and X. Wang, *Energy Environ. Sci.*, 2014, **7**, 2624–2629.
7. C. Wan, Y. Regmi and B. Leonard, *Angew. Chem. Int. Ed. Engl.*, 2014, **53**, 6407-6410.
8. M. Porosoff, X. Yang, J. Boscoboinik and J. G. Chen, *Angew. Chem. Int. Ed. Engl.*, 2014, **53**, 6705-6709.
9. J. Qiu, Z. Yang, Q. Li, Y. Li, X. Wu, C. Qi and Q. Qiao, *J. Mater. Chem. A*, 2016, **4**, 13296-13306.
10. X. Lv, J. Song, Y. Lai, J. Fang, J. Li and Z. Zhang, *J. Energy Storage*, 2016, **8**, 205-211.
11. M. Zhao, X. Xie, C. Ren, T. Makaryan, B. Anasori, G. Wang and Y. Gogotsi, *Adv. Mater.*, 2017, **29**, 1702410.

12. M. Li, S. Yu, Z. Chen, Z. Wang, F. Lv, B. Nan, Y. Zhu, Y. Shi, W. Wang, S. Wu, H. Liu, Y. Tang and Z. Lu, *Inorg. Chem. Front.*, 2017, **4**, 289-295.
13. X. Li, M. Deng, W. Zhang, Q. Gao, H. Wang, B. Yuan, L. Yang and M. Zhu, *Mater. Lett.*, 2017, **194**, 30-33.
14. H. Yu, H. Fan, J. Wang, Y. Zheng, Z. Dai, Y. Lu, J. Kong, X. Wang, Y. Kim, Q. Yan and J. Lee, *Nanoscale*, 2017, **9**, 7260-7267.
15. C. Wang, L. Sun, F. Zhang, X. Wang, Q. Sun, Y. Cheng and L. Wang, *Small*, 2017, **13**, 1701246.
16. W. Tian, H. Hu, Y. Wang, P. Li, J. Liu, J. Liu, X. Wang, X. Xu, Z. Li, Q. Zhao, H. Ning, W. Wu and M. Wu, *ACS Nano*, 2018, **12**, 1990-2000.
17. S. Niu, Z. Wang, M. Yu, M. Yu, L. Xiu, S. Wang, X. Wu and J. Qiu, *ACS Nano*, 2018, **12**, 3928-3937.
18. S. Liu, F. Li, D. Wang, C. Huang, Y. Zhao, J. Baek and J. Xu, *Small Methods*, 2018, **2**, 1800040.
19. J. Lin, J. Xu, W. Zhao, W. Dong, R. Li, Z. Zhang and F. Huang, *ACS Appl. Mater. Interfaces*, 2019, **11**, 19977-19985.
20. F. Lyu, S. Zeng, Z. Sun, N. Qin, L. Cao, Z. Wang, Z. Jia, S. Wu, F. Ma, M. Li, W. Wang, Y. Li, J. Lu and Z. Lu, *Small*, 2019, **15**, 1805022.